



**HAL**  
open science

## **A nanobody against the VWF A3 domain detects ADAMTS13-induced proteolysis in congenital and acquired VWD**

Claire Kizlik-Masson, Ivan Peyron, Stéphane Gangnard, Gaelle Le Goff, Solen Lenoir, Sandra Damodaran, Marie Clavel, Stéphanie Rouillet, Véronique Regnault, Antoine Rauch, et al.

► **To cite this version:**

Claire Kizlik-Masson, Ivan Peyron, Stéphane Gangnard, Gaelle Le Goff, Solen Lenoir, et al.. A nanobody against the VWF A3 domain detects ADAMTS13-induced proteolysis in congenital and acquired VWD. *Blood*, 2023, 141 (12), pp.1457-1468. 10.1182/blood.2022017569 . hal-04363218

**HAL Id: hal-04363218**

**<https://hal.science/hal-04363218>**

Submitted on 24 Dec 2023

**HAL** is a multi-disciplinary open access archive for the deposit and dissemination of scientific research documents, whether they are published or not. The documents may come from teaching and research institutions in France or abroad, or from public or private research centers.

L'archive ouverte pluridisciplinaire **HAL**, est destinée au dépôt et à la diffusion de documents scientifiques de niveau recherche, publiés ou non, émanant des établissements d'enseignement et de recherche français ou étrangers, des laboratoires publics ou privés.



American Society of Hematology  
2021 L Street NW, Suite 900,  
Washington, DC 20036  
Phone: 202-776-0544 | Fax 202-776-0545  
editorial@hematology.org

## **A nanobody against the von Willebrand factor A3-domain detects ADAMTS13-induced proteolysis in congenital & acquired VWD**

Tracking no: BLD-2022-017569R1

Claire Kizlik-Masson (INSERM, France) Ivan Peyron (INSERM U1176, France) Stéphane Gangnard (INSERM, France) Gaëlle Le Goff (Diagnostica Stago, France) Solen Lenoir (Diagnostica Stago, France) Sandra Damodaran (Diagnostica Stago, France) Marie Clavel (Inovarion, France) Rouillet Stephanie (INSERM, France) Veronique Regnault (Inserm, France) Antoine Rauch (CHU Lille, F-59000, France) Flavien Vincent (Univ. Lille, Inserm, CHU Lille, Institut Pasteur de Lille, U1011, EGID, F-59000 Lille, France, ) Emmanuelle Jeanpierre (CHU Lille, ) Annabelle Dupont (CHU Lille, France) Catherine TERNISIEN (CHU de Nantes, ) Thibault Donnet (Diagnostica Stago, France) Olivier Christophe (INSERM U1176, France) Eric Van Belle (Univ. Lille, Inserm, CHU Lille, Institut Pasteur de Lille, U1011, EGID, F-59000 Lille, France, ) Cecile Denis (INSERM, France) Caterina Casari (INSERM U1176, France) Sophie Susen (Lille University Hospital, France) Peter Lenting (INSERM, France)

### **Abstract:**

Von Willebrand factor (VWF) is a multimeric protein, the size of which is regulated via ADAMTS13-mediated proteolysis within the A2-domain. We aimed to isolate nanobodies distinguishing between proteolyzed and non-proteolyzed VWF, leading to the identification of a nanobody (designated KB-VWF-D3.1) targeting the A3-domain, the epitope of which overlaps the collagen-binding site. While KB-VWF-D3.1 binds with similar efficiency to dimeric and multimeric derivatives of VWF, binding to VWF was lost upon proteolysis by ADAMTS13, suggesting that proteolysis in the A2-domain modulates exposure of its epitope in the A3-domain. We therefore used KB-VWF-D3.1 to monitor VWF degradation in plasma samples. Spiking experiments showed that a loss of 10% intact-VWF could be detected using this nanobody. By comparing plasma from volunteers to that of congenital VWD-patients, intact-VWF levels were significantly reduced for all VWD-types, and most severely in VWD-type 2A-group 2 in which mutations promote ADAMTS13-mediated proteolysis. Unexpectedly, we also observed increased proteolysis in some patients with VWD-type 1 and VWD-type 2M. A significant correlation ( $r=0.51$ ,  $p<0.0001$ ) between the relative amount of high molecular weight-multimers and levels of intact-VWF was observed. Reduced levels of intact-VWF were further found in plasmas from patients with severe aortic stenosis and patients receiving mechanical circulatory support.

KB-VWF-D3.1 is thus a nanobody that detects changes in the exposure of its epitope within the collagen-binding site of the A3-domain. In view of its unique characteristics, it has the potential to be used as a diagnostic tool to investigate whether a loss of larger multimers is due to ADAMTS13-mediated proteolysis.

**Conflict of interest:** COI declared - see note

**COI notes:** GLF, SL, SD and TD are employees of Diagnostica Stago. The other authors declare no conflict of interest.

**Preprint server:** No;

**Author contributions and disclosures:** CKM, IP, SG, GLF, SML, SD, MC, SR, TD, CC and PJJ performed experiments and analyzed data; VR, AR, FV, EJ, AD, CT and EvB provided patient samples; SS, ODC, PJJ, CVD designed and supervised the study. All authors contributed to the interpretation of the data. PJJ wrote the first draft of the manuscript, and all authors contributed to the editing of the final manuscript.

**Non-author contributions and disclosures:** No;

**Agreement to Share Publication-Related Data and Data Sharing Statement:** Data are available upon reasonable request to the corresponding author

Clinical trial registration information (if any):

1 **A nanobody against the von Willebrand factor A3-domain detects ADAMTS13-induced**  
2 **proteolysis in congenital & acquired VWD**  
3

4 Claire Kizlik-Masson<sup>1,\*</sup>, Ivan Peyron<sup>1,\*</sup>, Stéphane Gangnard<sup>1</sup>, Gaëlle Le Goff<sup>2</sup>, Solen M  
5 Lenoir<sup>2</sup>, Sandra Damodaran<sup>2</sup>, Marie Clavel<sup>3</sup>, Stéphanie Rouillet<sup>1</sup>, Véronique Regnault<sup>4</sup>,  
6 Antoine Rauch<sup>5</sup>, Flavien Vincent<sup>5</sup>, Emmanuelle Jeanpierre<sup>5</sup>, Annabelle Dupont<sup>5</sup>, Catherine  
7 Ternisien<sup>6</sup>, Thibault Donnet<sup>2</sup>, Olivier D. Christophe<sup>1</sup>, Eric van Belle<sup>5</sup>, Cécile V. Denis<sup>1</sup>,  
8 Caterina Casari<sup>1</sup>, Sophie Susen<sup>5,6</sup>, Peter J. Lenting<sup>1</sup>  
9

10 <sup>1</sup>Laboratory for Hemostasis, Inflammation & Thrombosis, Unité Mixed de Recherche 1176,  
11 Institut National de la Santé et de la Recherche Médicale, Université Paris-Saclay, 94276 Le  
12 Kremlin-Bicêtre, France

13 <sup>2</sup>Diagnostica Stago, Unités de recherche & développement, Gennevilliers, France

14 <sup>3</sup>Inovation, Paris, France

15 <sup>4</sup>Université de Lorraine, Laboratory for Acute and Chronic Cardiovascular Deficiency  
16 (DCAC), Institut National de la Santé et de la Recherche Médicale Unité 1116, Nancy,  
17 France

18 <sup>5</sup>Université de Lille, Centre Hospitalier Universitaire Lille, Institut Pasteur de Lille, Institut  
19 National de la Santé et de la Recherche Médicale Unité 1011, Lille, France

20 <sup>6</sup>French Reference Center for von Willebrand disease (CRMW), Lille, France  
21

22 Authorship Contributions: CKM, IP, SG, GLF, SML, SD, MC, SR, TD, CC and PJJ performed  
23 experiments and analyzed data; VR, AR, FV, EJ, AD, CT and EvB provided patient samples;  
24 SS, ODC, PJJ, CVD designed and supervised the study. All authors contributed to the  
25 interpretation of the data. PJJ wrote the first draft of the manuscript, and all authors  
26 contributed to the editing of the final manuscript.  
27

28 \*CKM and IP contributed equally to this manuscript.  
29

30 **Correspondence:**

31 Peter J. Lenting, Inserm U1176, 80 rue du Général Leclerc, 94270 Le Kremlin-Bicêtre,  
32 France

33 Tel: +331-49595600; Fax: +33146719472; Email: peter.lenting@inserm.fr  
34

35 **Running title:** An anti-A3 domain nanobody detecting intact-VWF  
36

1 **Data sharing statement:** Data are available upon reasonable request to the corresponding  
2 author

3

4 **Word count:** 3972; **Abstract:** 250; **References:** 36; **Figures:** 6

5

6

1 **Key points**

2 Nanobody KB-VWF-D3.1 binds to the collagen-binding site in the VWF A3-domain, and  
3 loses its binding upon proteolysis of VWF by ADAMTS13

4

5 KB-VWF-D3.1 identified VWF degradation in VWD-patients, which correlated with a loss of  
6 larger VWF-multimers

7

8 **Abstract**

9 Von Willebrand factor (VWF) is a multimeric protein, the size of which is regulated via  
10 ADAMTS13-mediated proteolysis within the A2-domain. We aimed to isolate nanobodies  
11 distinguishing between proteolyzed and non-proteolyzed VWF, leading to the identification of  
12 a nanobody (designated KB-VWF-D3.1) targeting the A3-domain, the epitope of which  
13 overlaps the collagen-binding site. While KB-VWF-D3.1 binds with similar efficiency to  
14 dimeric and multimeric derivatives of VWF, binding to VWF was lost upon proteolysis by  
15 ADAMTS13, suggesting that proteolysis in the A2-domain modulates exposure of its epitope  
16 in the A3-domain. We therefore used KB-VWF-D3.1 to monitor VWF degradation in plasma  
17 samples. Spiking experiments showed that a loss of 10% intact-VWF could be detected  
18 using this nanobody. By comparing plasma from volunteers to that of congenital VWD-  
19 patients, intact-VWF levels were significantly reduced for all VWD-types, and most severely  
20 in VWD-type 2A-group 2 in which mutations promote ADAMTS13-mediated proteolysis.  
21 Unexpectedly, we also observed increased proteolysis in some patients with VWD-type 1  
22 and VWD-type 2M. A significant correlation ( $r=0.51$ ,  $p<0.0001$ ) between the relative amount  
23 of high molecular weight-multimers and levels of intact-VWF was observed. Reduced levels  
24 of intact-VWF were further found in plasmas from patients with severe aortic stenosis and  
25 patients receiving mechanical circulatory support.

26 KB-VWF-D3.1 is thus a nanobody that detects changes in the exposure of its epitope within  
27 the collagen-binding site of the A3-domain. In view of its unique characteristics, it has the  
28 potential to be used as a diagnostic tool to investigate whether a loss of larger multimers is  
29 due to ADAMTS13-mediated proteolysis.

30

1

## 2 **Introduction**

3 Von Willebrand factor is a multimeric protein, the extent of which regulates its interaction  
4 with platelets. Multimerization of VWF occurs during its synthesis in megakaryocytes or  
5 endothelial cells.<sup>1,2</sup> In this process, two VWF subunits (with the domain structure: D1-D2-D'  
6 D3-A1-A2-A3-D4-C1-C2-C3-C4-C5-C6-CK) are first covalently linked via disulfide bridging  
7 between two C-terminal CK-domains. These pro-dimers are then processed into multimers  
8 via N-terminal coupling of the D'-D3 regions, with the D1-D2 portion (also known as VWF  
9 propeptide) being eliminated during this event. The multimer size in endothelial cells is highly  
10 variable and varies from dimers to ultra-large multimers with >40 subunits. Upon secretion,  
11 VWF multimers are susceptible to regulated proteolysis by ADAMTS13, a metalloprotease  
12 that cleaves VWF in its A2-domain at the Tyr<sup>1605</sup>-Met<sup>1606</sup> peptide bond.<sup>3</sup> Importantly,  
13 proteolysis occurs only upon decryption of the cleavage site, which normally lies buried  
14 within the A2-domain.<sup>4</sup>

15 There are several occurrences that allow for the exposure of the ADAMTS13-cleavage site.  
16 First, multiple VWF multimers assemble at the endothelial surface upon stimulated secretion,  
17 forming elongated fibers that are proteolyzed by ADAMTS13.<sup>5-7</sup> Second, VWF unfolds during  
18 circulation under conditions of increased shear stress or disturbed blood flow.<sup>8</sup> When  
19 disturbed blood flow is exaggerated, like in patients having severe aortic stenosis or those  
20 who require mechanical circulatory support, excessive VWF degradation may occur, which is  
21 then referred to as acquired von Willebrand syndrome (AVWS).<sup>9-11</sup> Third, mutations within  
22 VWF may provoke exposure of the ADAMTS13 proteolytic site, and such mutations are most  
23 frequently found in von Willebrand disease (VWD)-type 2A-group 2 and VWD-type 2B.<sup>12,13</sup>

24 Excessive proteolysis of VWF is associated with an increased loss of high molecular weight  
25 (HMW)-multimers, which results in reduced platelet binding and reduced collagen binding,  
26 thereby increasing the risk of bleeding.<sup>9</sup> The classic approach to visualize the extent of VWF  
27 degradation is to analyze the multimeric pattern using SDS-agarose electrophoresis.<sup>14</sup> This  
28 approach is laborious, non-standardized and requires 24-72h, dependent on the method that  
29 is used. Alternatively, collagen- or platelet-binding assays are used<sup>15</sup>, which are less specific  
30 in that they do not distinguish between impaired multimerization and excessive degradation.  
31 Finally, Kato and colleagues described a monoclonal antibody that binds to the newly formed  
32 C-terminal end in the A2-domain (residues Asp<sup>1596</sup>-Tyr<sup>1605</sup>). This antibody was successfully  
33 used to measure ADAMTS13 activity in patients with thrombotic thrombocytopenic  
34 purpura.<sup>16</sup> In addition, we and others used this antibody to monitor VWF proteolysis in  
35 patients.<sup>17,18</sup> However, while using an antibody targeting residues Asp<sup>1596</sup>-Tyr<sup>1605</sup>, we noticed  
36 that this antibody was unable to detect degradation, for instance in samples from patients  
37 with non-severe aortic stenosis or with congenital VWD-type 1 or 2M.

1 In the present study, we have developed a nanobody (designated KB-VWF-D3.1) that  
2 distinguishes between intact and ADAMTS13-cleaved VWF. Interestingly, this nanobody  
3 binds to the A3-domain, showing that proteolysis within the A2-domain modifies the  
4 exposure of the nanobody's epitope in the adjacent A3-domain. This nanobody proved  
5 sensitive to detect degradation in plasma from patients with AVWS and congenital VWD,  
6 including types 1 and 2M.

7

8



1 **Materials & methods**

2 An extensive description of the experimental procedures can be found in the Supplementary  
3 methods (available on the *Blood* website).

4

5 *Ethics statement:*

6 All volunteers and patients provided informed written consent according to the Declaration of  
7 Helsinki. Patients with VWD were selected from the French cohort multicentric database of  
8 VWD (Centre Reference Maladie Willebrand).<sup>19</sup> The database and biobank of this cohort are  
9 declared to and approved by the French data protection authority (CNIL-1245379/DEC-  
10 19252, CODECOH-DC-2008-642). Patients with severe aortic stenosis (WITAVI-trial,  
11 NCT02628509) and patients receiving extracorporeal mechanical oxidation (ECMO;  
12 WITECMO-H-trial; NCT03070912) were included in the study. All protocols were approved  
13 by the local review and ethics committees.

14

15 *Isolation of anti-VWF nanobodies*

16 A synthetic nanobody-encoding phage-library<sup>20</sup> was used to isolate anti-VWF nanobodies.  
17 The library ( $3 \times 10^9$  clones) was incubated with streptavidin-coated beads loaded with  
18 biotinylated rVWF. Unbound phages were then incubated with beads loaded with  
19 biotinylated degraded-VWF. Three rounds of phage-display were performed, with the  
20 depletion step being repeated every round. Twelve unique sequences were obtained via this  
21 procedure (Fig. 1A).

22

23 *Analysis of VWF binding to nanobodies*

24 Wells coated with nanobody KB-VWF-D3.1 or KB-VWF-1.1 (both 5  $\mu\text{g/ml}$ ) were incubated  
25 with purified rVWF (0-0.5  $\mu\text{g/ml}$ ). Bound VWF was probed using polyclonal anti-VWF  
26 antibodies and detected via hydrolysis of 3,3',5,5'-tetramethylbenzidine.

27

28 *Detecting intact-VWF*

29 Intact-VWF is referred as VWF being recognized by KB-VWF-D3.1. Briefly, wells coated with  
30 KB-VWF-D3.1 (5  $\mu\text{g/ml}$ ) were incubated with samples containing non-proteolyzed VWF,  
31 ADAMTS13-proteolyzed VWF or a mixture of both. Alternatively, plasma samples were  
32 used. Bound VWF was probed using polyclonal anti-VWF antibodies and detected via  
33 hydrolysis of 3,3',5,5'-tetramethylbenzidine.

34

35 *Total VWF-antigen*

1 Total VWF-antigen was measured in an elisa using polyclonal rabbit anti-VWF antibodies as  
2 described.<sup>21</sup>  
3

## 1 **Results**

### 2 *Selection of anti-VWF nanobodies*

3 To isolate nanobodies that distinguish between intact or proteolyzed VWF, a selection  
4 method using rVWF and degraded-VWF was applied, generating 12 unique sequences  
5 (Figure 1A-C). Purified nanobodies were tested for interaction with rVWF and degraded-  
6 VWF. Whereas 10 of 12 nanobodies displayed similar binding to both VWF preparations,  
7 two of them were characterized by differential binding. First, rVWF associated in a dose-  
8 dependent manner to immobilized nanobody KB-VWF-D3.1, whereas binding of degraded-  
9 VWF to this nanobody was strongly reduced (Figure 1D). In these assays, pd-VWF yielded  
10 responses that were consistently lower than rVWF (93±4% compared to 100±2%; p=0.015;  
11 Figure 1E), probably due to degraded-VWF present in normal plasma. In complementary  
12 assays, KB-VWF-D3.1 bound 8-fold less efficiently to immobilized degraded-VWF compared  
13 to immobilized rVWF (Supplementary figure S1). As for KB-VWF-F1.1, efficient binding of  
14 degraded-VWF was detected, whereas binding of rVWF approached background levels  
15 (Figure 1F). Therefore, these two nanobodies were selected for further analysis.

16

### 17 *Determination of the binding epitope for KB-VWF-F1.1*

18 Since KB-VWF-F1.1 bound to degraded-VWF but not intact-VWF, we anticipated that this  
19 nanobody recognizes the region surrounding the Tyr<sup>1605</sup>-Met<sup>1606</sup> cleavage site. This was  
20 tested in an ADAMTS13-activity test utilizing its substrate FRETs-VWF73, which contains  
21 the VWF A2-domain sequence Asp<sup>1596</sup>-Arg<sup>1668</sup> (Supplemental figure S2A). Whereas KB-  
22 VWF-D3.1 and control nanobody KB-VWF-004 (against the region VWF/D4-CK) left  
23 substrate proteolysis unaffected, KB-VWF-F1.1 efficiently interfered with substrate  
24 conversion by ADAMTS13. This suggests that the epitope of VWF-KB-F1.1 is located within  
25 the region Asp<sup>1596</sup>-Arg<sup>1668</sup>. Of note, KB-VWF-F1.1 and MAB27642, which targets residues  
26 Arg<sup>1596</sup>-Tyr<sup>1605</sup>, did not compete for binding to degraded-VWF (Supplementary figure S2B),  
27 suggesting they recognize different epitopes within this region.

28

### 29 *Determination of the binding epitope for KB-VWF-D3.1*

30 To determine the epitope of KB-VWF-D3.1, we first analyzed binding of this nanobody to a  
31 series of rVWF fragments, *ie.* A1-Fc, A2-Fc, A3-Fc and D4-Fc. Surprisingly, KB-VWF-D3.1  
32 bound most efficiently to the A3-Fc fragment rather than the A2-Fc (Figure 2A). Binding was  
33 similar when binding of fragments to immobilized KB-VWF-D3.1 was assessed  
34 (Supplementary figure S3A). Moreover, no binding of rVWF lacking the A3 domain to KB-  
35 VWF-D3.1 could be detected, whereas deletion of other domains left binding unaffected  
36 (Supplementary figure S3B).

1 To refine its binding site within the A3-domain, molecular modeling was performed (see  
2 supplementary materials). This procedure revealed that the top 30-ranked conformations of  
3 the complex all clustered similarly, with the nanobody docking onto 4 separate amino acid-  
4 stretches within the VWF A3-domain region Val<sup>1731</sup>-Asn<sup>1818</sup> (Figure 2B-D). Interestingly, 8 of  
5 the amino acids included in the epitope of KB-VWF-D3.1 have previously been recognized  
6 as being relevant for collagen binding (Figure 2E)<sup>22</sup>, indicating that the epitope of KB-VWF-  
7 D3.1 overlaps the collagen binding site. Consequently, we compared the effect of KB-VWF-  
8 D3.1 to that of two known A3-domain binding antibodies (the C37h nanobody<sup>23</sup> and the  
9 Mab505 monoclonal antibody<sup>24</sup>) on binding of VWF to collagen type III. The positive controls  
10 C37h and Mab505 efficiently blocked pd-VWF-collagen interactions (Figure 2F). KB-VWF-  
11 D3.1 also dose-dependently reduced binding of pd-VWF to collagen, but less efficiently than  
12 antibodies C37h and Mab505 (Figure 2F). In addition, KB-VWF-D3.1 delayed VWF-  
13 dependent platelet-adhesion to collagen under flow-conditions (Supplementary figure S3C).  
14 Having their epitope overlapping the collagen binding site in common, it raises the question  
15 whether C37h and Mab505 can distinguish between intact and degraded-VWF akin to KB-  
16 VWF-D3.1. However, both C37h and Mab505 displayed similar binding to both intact rVWF  
17 and degraded-VWF (Figure 2G). Thus, nanobody KB-VWF-D3.1 is unique in binding to an  
18 epitope within the A3-domain, the exposure of which is modulated upon proteolysis within  
19 the A2-domain.

20

#### 21 *Effect multimer size on VWF binding to KB-VWF-D3.1*

22 Proteolysis of VWF by ADAMTS13 results in loss of the Tyr<sup>1605</sup>-Met<sup>1606</sup> peptide bond, thereby  
23 reducing multimer size. We therefore tested how multimer size affects binding of VWF to  
24 immobilized KB-VWF-D3.1. First, we analyzed two distinct pd-VWF preparations that were  
25 obtained from pd-VWF concentrates via gel-filtration chromatography. One with HMW-  
26 multimers and one enriched in medium-sized molecular weight multimers (Figure 3A). Both  
27 fractions displayed similar binding to KB-VWF-D3.1 (Figure 3B). Next, we compared binding  
28 of dimeric rVWF/delta-pro to that of full-length rVWF (Figure 3C). Both dimeric rVWF/delta-  
29 pro and rVWF bound to KB-VWF-D3.1 with similar half-maximal binding ( $0.2 \pm 1 \mu\text{g/ml}$  vs  
30  $0.2 \pm 0.1 \mu\text{g/ml}$ ;  $p=0.62$ ). Apparently, binding of VWF to immobilized KB-VWF-D3.1 is  
31 independent of its multimer size. Reduced binding of degraded-VWF to KB-VWF-D3.1 is  
32 conceivably originating from proteolysis of the Tyr<sup>1605</sup>-Met<sup>1606</sup> peptide bond rather than from  
33 a reduction in multimer size.

34

#### 35 *Proteolysis of VWF over time*

1 We next investigated the effect of ADAMTS13-proteolysis on VWF binding to KB-VWF-D3.1  
2 and KB-VWF-F1.1 in a time-dependent manner. Briefly, pd-VWF was exposed to shear in  
3 the presence of recombinant ADAMTS13 and samples were taken at indicated time-points  
4 (0-3h). Multimeric pattern and binding to both nanobodies were analyzed. Exposure to  
5 ADAMTS13 resulted in a time-dependent decrease in pd-VWF multimer size (Figure 4A). As  
6 expected, proteolysis was inhibited in the presence of EDTA, a metal-ion chelator which  
7 renders ADAMTS13 inactive. Concurrent with increased pd-VWF proteolysis, increased  
8 binding to KB-VWF-F1.1 was observed (Figure 4B). In contrast, binding of pd-VWF to KB-  
9 VWF-D3.1 disappeared in a complementary fashion (Figure 4B). These data validate that  
10 the binding of both nanobodies to VWF is dependent on the extent of proteolysis by  
11 ADAMTS13.

12

### 13 *Measuring degraded-VWF in mixtures of intact and degraded-VWF*

14 Given the specificity of both nanobodies for intact and degraded-VWF, respectively, we  
15 anticipated that they could be useful to determine the extent of VWF proteolysis in patient  
16 samples. In preliminary experiments, KB-VWF-F1.1 lacked sufficient sensitivity to detect  
17 minor proteolysis of VWF in plasma, and we therefore focused for the remainder of the study  
18 on KB-VWF-D3.1. We first analyzed to what extent increased proteolysis would be  
19 detectable. Different mixtures of purified rVWF and degraded-VWF were prepared, and the  
20 ratio intact VWF/total VWF-antigen was determined. A dose-dependent decrease of this ratio  
21 was observed, when the percentage of degraded-VWF in the samples increased (Figure  
22 5A). From these experiments, it seems that an increase of approximately 10% degraded-  
23 VWF can be detected ( $p=0.0009$  compared 100% intact).

24

### 25 *Analysis of congenital VWD-patient plasma*

26 We then analyzed plasma samples obtained from controls ( $n=31$ ) and VWD-patients  
27 included in the French reference center for VWD ( $n=101$ ).<sup>19</sup> The patient-cohort consisted of  
28 VWD-type 1 ( $n=20$ ), VWD-type 2A ( $n=43$ ), VWD-type 2B ( $n=24$ ) and VWD-type 2M ( $n=14$ )  
29 patients.

30 To determine the amount of intact VWF, we calculated the amount of antigen obtained using  
31 KB-VWF-D3.1 (= intact-VWF) over the amount of total VWF-antigen, using normal pooled  
32 plasma as calibrator. By doing so, it appeared that the intact-VWF/total antigen ratio for  
33 controls was found to be  $1.0\pm 0.2$  (Figure 5B). The ratio of intact-VWF/total VWF was  
34 decreased for each of the VWD-types analyzed. The ratio was  $0.7\pm 0.3$  ( $p=0.0004$ ) for VWD-  
35 type 1,  $0.5\pm 0.2$  ( $p<0.0001$ ) for VWD-type 2A,  $0.6\pm 0.2$  ( $p<0.0001$ ) for VWD-type 2B and  
36  $0.7\pm 0.2$  ( $p=0.0148$ ) for VWD-type 2M (Figure 5B). A separate graph showing the ratio for  
37 each mutation is presented in the Supplementary figure S4. Since VWD-type 2A is divided in

1 two subtypes, *ie.* VWD-type 2A-group 1 and VWD-type 2A-group 2, in which the loss of  
2 multimers is dominated by impaired multimerization and increased proteolysis, respectively,  
3 we separately analyzed samples from patients with VWD-type 2A-group 1 (n=14) and VWD-  
4 type 2A-group 2 (n=29). The ratio intact-VWF/total VWF-antigen was significantly lower in  
5 VWD-type 2A-group 2 ( $0.4\pm 0.2$ ) compared to VWD-type 2A-group 1 ( $0.6\pm 0.2$ ;  $p=0.0007$ ;  
6 Figure 5C).

7 Since it was unexpected to find a decreased ratio intact-VWF/total VWF-antigen in all VWD-  
8 types, we also verified whether this decreased ratio would correspond to a potential loss of  
9 HMW-multimers. Multimer analysis was available for a subset of samples, and we indeed  
10 observed that in all patient groups, including VWD-type 1 and type 2M, there was on  
11 average a relative decrease in the HMW-multimers (>10 multimer bands) compared to  
12 normal pooled plasma, (Figure 5D). An example of a multimeric pattern with reduced HMW-  
13 multimers for a VWD-type 1 and type 2M patient is provided in Supplementary figure S5.  
14 Interestingly, there was a significant correlation between the ratio intact-VWF/total VWF-  
15 antigen *versus* multimer size ( $r=0.51$ ;  $p<0.0001$ ; Figure 5E). Thus, it seems that in the  
16 majority of VWD-patients there is increased proteolysis compared to the normal population.

17

#### 18 *Analysis of AVWS-patient plasma*

19 We next examined plasma from patients receiving ECMO-support (n=27) and from patients  
20 with severe aortic stenosis (n=17). Both patient groups are characterized by a loss of VWF  
21 HMW-multimers (Figure 6A), potentially caused by increased ADAMTS13-mediated  
22 proteolysis. Compared to normal control, the ratio of intact-VWF (measured by binding to  
23 KB-VWF-D3.1) over total VWF-antigen was significantly reduced for both patient groups:  
24  $0.85\pm 0.09$  (mean $\pm$ SD;  $p=0.0017$ ) and  $0.78\pm 0.13$  ( $p<0.0001$ ) for severe aortic stenosis and  
25 ECMO patients, respectively (Figure 6B). Of note, for both groups, there was a significant  
26 correlation between the ratio intact/total antigen and the presence of HMW-multimers (>10),  
27 with p-values being  $p=0.0463$  for severe aortic stenosis-samples and  $p=0.0452$  for ECMO-  
28 samples (Figures 6C-D). This may suggest that the loss of larger multimers indeed is  
29 predominantly due to proteolysis rather than other mechanisms.

30

1 **Discussion**

2 In this study, we describe a novel nanobody, designated KB-VWF-D3.1, that loses its  
3 capacity to bind VWF upon proteolysis by ADAMTS13. We show that this nanobody displays  
4 reduced binding to VWF present in plasma of congenital VWD patients as well in those  
5 having an acquired deficiency of VWF. Unexpectedly, this nanobody revealed the presence  
6 of increased VWF degradation in some patients with VWD-type 1 and 2M.

7 Structural conformational changes are key regulators of VWF function. Although there are  
8 several ways to monitor such structural changes, including functional assays and  
9 microscopic visualization, the use of specific antibodies is by far the most convenient and  
10 accessible approach. In 2005, a nanobody (AU-VWFa-11) was described that selectively  
11 binds to VWF in its active, glycoprotein I $\beta$ -binding conformation, but not to globular inactive  
12 VWF.<sup>25</sup> This nanobody has indeed been useful to identify the presence of active VWF under  
13 several pathological conditions.<sup>26-31</sup> Following a similar strategy, we set out to identify  
14 nanobodies that distinguish between intact and ADAMTS13-proteolyzed VWF, leading to the  
15 successful identification of a nanobody that binds to intact- but not to degraded-VWF (Figure  
16 1).

17 Admittedly, others have reported antibodies that distinguish intact- and degraded-VWF.<sup>16,32</sup>  
18 These antibodies have in common that they recognize the VWF A2-domain and only bind  
19 VWF in its elongated or proteolyzed conformation. Our nanobody is different from these  
20 antibodies in two distinct ways: first, it binds to VWF in both globular and elongated  
21 conformations (allowing it to detect intact-VWF in plasma samples), and second by having  
22 its epitope in the VWF A3-domain. Of course, binding to the A3-domain is perhaps less  
23 relevant from a diagnostic point of view, but its unique epitope may provide new insights into  
24 the structure-function relationship of VWF. Indeed, the identification of the epitope of KB-  
25 VWF-D3.1 being in the A3-domain was unexpected in the sense that proteolysis of VWF by  
26 ADAMTS13 takes place in the adjacent A2-domain. Nevertheless, a series of experiments  
27 undoubtedly led to the conclusion that KB-VWF-D3.1 indeed interacts with the A3-domain,  
28 and more specifically, that its epitope overlaps the collagen binding site (Figure 2;  
29 supplementary figure S3).

30 The notion that KB-VWF-D3.1 binds to the A3-domain clearly raises the question how  
31 proteolysis in the A2-domain may affect the exposure of the epitope of KB-VWF-D3.1 in the  
32 A3-domain? It has previously been shown that different domains within VWF can interact or  
33 communicate with each other. For instance, VWF has a 4-fold reduced affinity for FVIII when  
34 bound to collagen, suggesting that binding of the A3-domain to collagen affects the  
35 exposure of the FVIII binding site in the D'D3-region.<sup>33</sup> It is thus possible that proteolysis  
36 within the A2-domain may result in conformational changes in the A3-domain. Second, the  
37 D'D3-region and the A2-domain can both bind to the A1-domain.<sup>34,35</sup> From this perspective,

1 the possibility exists that proteolysis in the A2-domain allows a portion of this domain to  
2 move towards the A3-domain, binding to the adjacent epitope of KB-VWF-D3.1. Irrespective  
3 of the exact mechanism, given that this epitope overlaps the collagen binding site, it is  
4 tempting to speculate that there exists an additional mechanism by which ADAMTS13  
5 reduces the hemostatic potential of VWF: not only would proteolysis reduce multimer size,  
6 but modulating the exposure of the collagen binding site could reduce the capacity of VWF  
7 to bind collagen. In this scenario, the ratio affected A3-domains/normal A3-domains would  
8 be determinant for the extent by which collagen binding is modulated. Additional  
9 experiments are warranted to explore this hypothesis in more detail.

10 Should the cleaved A2-domain indeed start covering the epitope of KB-VWF-D3.1, then this  
11 may also provide a possible explanation why KB-VWF-D3.1 but not the concurrent  
12 antibodies C37h and Mab505 distinguishes between intact and degraded VWF. Both  
13 antibodies have a significant higher affinity for VWF. As such, they would efficiently compete  
14 with the A2-domain for a common binding site within the A3-domain, and therefore be  
15 unable to detect proteolysis within the A2-domain.

16 Between both nanobodies KB-VWF-D3.1 and KB-VWF-F1.1, the former proved most  
17 sensitive in detecting degradation of VWF. Both monovalent and bivalent variants of KB-  
18 VWF-F1.1 did bind degraded VWF only at relatively high concentrations. In this respect, KB-  
19 VWF-F1.1 seems similar to the antibody described by Kato and coworkers.<sup>16</sup> It is possible  
20 that the low affinity originates from the flexible nature of their epitope, the polypeptides at  
21 either end of the Tyr<sup>1605</sup>-Met<sup>1606</sup> cleavage site.

22 Focusing on nanobody KB-VWF-D3.1, we investigated whether this nanobody could detect  
23 increased proteolysis in samples of patients. To do so, the nanobody should meet with a  
24 number of criteria: 1. binding should be independent of multimer size; 2. binding should  
25 decrease dose-dependently upon an increased presence of proteolyzed VWF; and 3. the  
26 nanobody should be sufficiently sensitive to detect low amounts of proteolyzed VWF. By  
27 performing a number of control experiments, it seems that KB-VWF-D3.1 indeed meets  
28 these three criteria (Fig. 3-5). In particular, the notion that the presence of 10% degraded-  
29 VWF could be detected is relevant.

30 Although this study has not been designed to validate the KB-VWF-D3.1-based assay as a  
31 diagnostic tool, we did analyze a series of control and patient samples. We measured both  
32 the amount of antigen detected using KB-VWF-D3.1 (referred to as intact-VWF) and the  
33 amount of antigen using polyclonal anti-VWF antibodies (referred to as total VWF-antigen).  
34 When analyzing 31 control samples from volunteers, the ratio intact-VWF/total VWF-antigen  
35 was  $1.0 \pm 0.2$  (mean  $\pm$  SD), with a 95% confidence interval being 0.9-1.1 (Figure 5). A few of  
36 these samples were either particularly low with a ratio  $< 0.82$  (mean - 1xSD; 3 out of 31  
37 samples) or particularly high ( $> 1.20$ ; mean + 1xSD; 4/31 samples). Apparently, on average,



1 the analyzed individual plasma samples do not contain less intact-VWF compared to the  
2 plasma calibrator. However, there exists within this control group a number of individuals in  
3 which proteolysis of VWF seems somewhat up- or down-regulated.

4 We also had access to a large group of congenital VWD-patients. As expected, the intact-  
5 VWF/total VWF-antigen ratio was lowest in samples from VWD-type 2A-group 2 patients,  
6 who express mutated VWF that has increased sensitivity for ADAMTS13-mediated  
7 proteolysis.<sup>12</sup> Also for VWD-type 2B it has been reported that ADAMTS13 may contribute to  
8 the loss of larger multimers in these patients, but this degradation is very much mutation  
9 dependent.<sup>13</sup> Indeed, ratios between 0.14 and 1.03 were obtained in these samples,  
10 suggesting a high variability between VWD-type 2B patients. Unexpectedly, we also  
11 observed a decreased ratio intact-VWF/total VWF-antigen in part of patients with VWD-type  
12 1 and VWD-type 2M, although to a lesser extent compared to VWD-type 2A and 2B. This  
13 suggests that there is an increase in VWF degradation in these samples compared to normal  
14 controls. If so, one would anticipate that there is a concordant loss of HMW-multimers. We  
15 indeed observed that compared to normal pooled plasma, all subtypes including VWD-type 1  
16 and VWD-type 2M samples were characterized by reduced quantities of the larger multimers  
17 (Figure 5). Moreover, there was a highly significant correlation between the ratio intact  
18 VWF/total VWF-antigen and the presence of these larger multimers. It seems conceivable  
19 therefore that at least part of the loss of HMW-multimers can be explained by an increased  
20 degradation of VWF by ADAMTS13.

21 It is of interest to mention that we noticed quite some variation in the extent of VWF  
22 degradation in patients with a similar mutation (Supplementary figure S4). This suggests that  
23 besides the mutation itself, also other factors may contribute to the extent by which VWF is  
24 proteolyzed by VWF. One potential hypothesis could be that mutations allow VWF to unfold  
25 more easily during circulation, for instance at sites of bifurcations, making them more  
26 susceptible to proteolysis. This effect would be amplified if secondary conditions, like a  
27 developing atherosclerosis, further contribute to the presence of disturbed flow conditions.  
28 Whether this will be associated with a more pronounced bleeding phenotype remains to be  
29 investigated.

30 Excessive VWF degradation associated with a loss of HMW-multimers is also observed in  
31 AVWS, including in patients with severe aortic stenosis and ECMO-patients (Figure 6). It  
32 was perhaps unsurprising therefore that levels of intact-VWF were significantly reduced in  
33 both patient groups. As for the congenital VWD samples, both AVWS groups displayed a  
34 significant correlation between the ratio intact-VWF/total VWF-antigen and the presence of  
35 larger multimers. Importantly, the average loss of intact-VWF was less pronounced in severe  
36 aortic stenosis and ECMO-patients compared to congenital VWD-patients.

1 We noted that degradation of VWF was more pronounced in VWD-type 2A-group 2 patients  
2 and *in vitro* degradation-assays compared to AVWS patients, although all are exposed to  
3 conditions that favor VWF degradation. This difference can be explained by the fact that  
4 VWF is constitutively in a ADAMTS13-sensitive conformation in VWD-type 2A-group 2 and  
5 in the *in vitro* degradation assays, allowing both large and short multimers to be proteolyzed.  
6 In contrast, in AVWS, VWF is elongated during a short period of time, when passing the  
7 stenosed valve or the mechanic pump. Such conditions particularly favor proteolysis of the  
8 larger multimers only, with the highest chances of cleavage occurring within the middle  
9 region of these multimers (Supplementary figure S6).

10 Taken together, we have developed a novel nanobody that binds to the A3-domain of VWF,  
11 a subunit that is not proteolyzed by ADAMTS13. This nanobody not only provided new  
12 insight into how ADAMTS13 may regulate the exposure of the collagen binding site within  
13 the A3-domain, but it also identified the presence of low-grade VWF degradation in a large  
14 amount of patient samples. By using its sensitivity, we revealed an increase in VWF  
15 degradation in VWD-type 1 and 2M samples, which we were unable to do with assays  
16 currently available for detecting degraded-VWF.

17 Whether KB-VWF-D3.1 could be useful as a diagnostic tool regarding congenital VWD  
18 would need to be established in additional studies designed for this specific purpose.  
19 However, we anticipate that our assay might be useful in a number of other situations. First,  
20 we now that in the majority of aortic stenosis patients that undergo transcatheter valve  
21 replacement, the VWF degradation defect is corrected within 5-10 minutes after valve  
22 placement.<sup>11,36</sup> However, the VWF degradation defect is not corrected in 10-20% of the  
23 patients due to incorrect valve placement that causes regurgitation. Currently, no point-of-  
24 care assays are available to verify the correct placement of the valves. It is possible that a  
25 point-of-care assay using KB-VWF-D3.1 could be applied for this purpose, as it will detect an  
26 increase in levels of intact-VWF. Second, this rapid point-of-care approach can also be used  
27 to test the opposite, *ie.* if there is loss of VWF degradation due to a lack of ADAMTS13  
28 activity. This could eventually facilitate the clinical decision-making of patients that arrive into  
29 the hospital with suspected thrombotic thrombocytopenic purpura.

30  
31  
32  
33  
34

1 **Funding:** This study received funding from the National Research Agency (Agence  
2 Nationale de la Recherche, grant numbers ANR-17-RHUS-17-0011-WIIIAssistHeart and  
3 ANR-21-CE14-0076-02-Vista) and the foundation Crédit Agricole Nord de France.

4

5 **Acknowledgements:** The authors thank Drs. Jenny Goudemand, Edith Fressinaud,  
6 Mouhamed Moussa, Christophe Zawadzki and Pierre Boisseau for the development, patient  
7 recruitment and genetic analysis of the patient cohort in the framework of the CRMW.

8

9 **Conflict of interest:** GLF, SL, SD and TD are employees of Diagnostica Stago. The other  
10 authors declare no conflict of interest.

11

12

## 1   **References**

- 2   1. Springer TA. von Willebrand factor, Jedi knight of the bloodstream. *Blood*.  
3       2014;124(9):1412-1425.
- 4   2. Lenting PJ, Christophe OD, Denis CV. von Willebrand factor biosynthesis, secretion,  
5       and clearance: connecting the far ends. *Blood*. 2015;125(13):2019-2028.
- 6   3. Levy GG, Nichols WC, Lian EC, et al. Mutations in a member of the ADAMTS gene  
7       family cause thrombotic thrombocytopenic purpura. *Nature*. 2001;413(6855):488-494.
- 8   4. Crawley JT, de Groot R, Xiang Y, Luken BM, Lane DA. Unraveling the scissile bond:  
9       how ADAMTS13 recognizes and cleaves von Willebrand factor. *Blood*.  
10      2011;118(12):3212-3221.
- 11  5. Dong JF, Moake JL, Nolasco L, et al. ADAMTS-13 rapidly cleaves newly secreted  
12      ultralarge von Willebrand factor multimers on the endothelial surface under flowing  
13      conditions. *Blood*. 2002;100(12):4033-4039.
- 14  6. De Ceunynck K, De Meyer SF, Vanhoorelbeke K. Unwinding the von Willebrand factor  
15      strings puzzle. *Blood*. 2013;121(2):270-277.
- 16  7. De Ceunynck K, Rocha S, Feys HB, et al. Local elongation of endothelial cell-anchored  
17      von Willebrand factor strings precedes ADAMTS13 protein-mediated proteolysis. *J Biol*  
18      *Chem*. 2011;286(42):36361-36367.
- 19  8. Springer TA. Biology and physics of von Willebrand factor concatamers. *J Thromb*  
20      *Haemost*. 2011;9 Suppl 1:130-143.
- 21  9. Vincentelli A, Susen S, Le Tourneau T, et al. Acquired von Willebrand syndrome in  
22      aortic stenosis. *N Engl J Med*. 2003;349(4):343-349.
- 23  10. Van Belle E, Rauch A, Vincentelli A, et al. Von Willebrand factor as a biological sensor  
24      of blood flow to monitor percutaneous aortic valve interventions. *Circ Res*.  
25      2015;116(7):1193-1201.
- 26  11. Vincent F, Rauch A, Loobuyck V, et al. Arterial Pulsatility and Circulating von Willebrand  
27      Factor in Patients on Mechanical Circulatory Support. *J Am Coll Cardiol*.  
28      2018;71(19):2106-2118.
- 29  12. Haberichter SL, Fahs SA, Montgomery RR. von Willebrand factor storage and  
30      multimerization: 2 independent intracellular processes. *Blood*. 2000;96(5):1808-1815.
- 31  13. Rayes J, Hommais A, Legendre P, et al. Effect of von Willebrand disease type 2B and  
32      type 2M mutations on the susceptibility of von Willebrand factor to ADAMTS-13. *J*  
33      *Thromb Haemost*. 2007;5(2):321-328.
- 34  14. Budde U. Diagnosis of von Willebrand disease subtypes: implications for treatment.  
35      *Haemophilia*. 2008;14 Suppl 5:27-38.
- 36  15. Sharma R, Flood VH. Advances in the diagnosis and treatment of Von Willebrand  
37      disease. *Blood*. 2017;130(22):2386-2391.

- 1 16. Kato S, Matsumoto M, Matsuyama T, Isonishi A, Hiura H, Fujimura Y. Novel monoclonal  
2 antibody-based enzyme immunoassay for determining plasma levels of ADAMTS13  
3 activity. *Transfusion*. 2006;46(8):1444-1452.
- 4 17. Rauch A, Caron C, Vincent F, et al. A novel ELISA-based diagnosis of acquired von  
5 Willebrand disease with increased VWF proteolysis. *Thromb Haemost*.  
6 2016;115(5):950-959.
- 7 18. Kubo M, Sakai K, Hayakawa M, et al. Increased cleavage of von Willebrand factor by  
8 ADAMTS13 may contribute strongly to acquired von Willebrand syndrome development  
9 in patients with essential thrombocythemia. *J Thromb Haemost*. 2022.
- 10 19. Veyradier A, Boisseau P, Fressinaud E, et al. A Laboratory Phenotype/Genotype  
11 Correlation of 1167 French Patients From 670 Families With von Willebrand Disease: A  
12 New Epidemiologic Picture. *Medicine (Baltimore)*. 2016;95(11):e3038.
- 13 20. Moutel S, Bery N, Bernard V, et al. NaLi-H1: A universal synthetic library of humanized  
14 nanobodies providing highly functional antibodies and intrabodies. *Elife*. 2016;5:e16228.
- 15 21. Lenting PJ, Westein E, Terraube V, et al. An experimental model to study the in vivo  
16 survival of von Willebrand factor. Basic aspects and application to the R1205H mutation.  
17 *J Biol Chem*. 2004;279(13):12102-12109.
- 18 22. Romijn RA, Westein E, Bouma B, et al. Mapping the collagen-binding site in the von  
19 Willebrand factor-A3 domain. *J Biol Chem*. 2003;278(17):15035-15039.
- 20 23. Wohner N, Sebastian S, Muczynski V, et al. Osteoprotegerin modulates platelet  
21 adhesion to von Willebrand factor during release from endothelial cells. *J Thromb  
22 Haemost*. 2022;20(3):755-766.
- 23 24. Navarrete AM, Casari C, Legendre P, et al. A murine model to characterize the  
24 antithrombotic effect of molecules targeting human von Willebrand factor. *Blood*.  
25 2012;120(13):2723-2732.
- 26 25. Hulstein JJ, de Groot PG, Silence K, Veyradier A, Fijnheer R, Lenting PJ. A novel  
27 nanobody that detects the gain-of-function phenotype of von Willebrand factor in  
28 ADAMTS13 deficiency and von Willebrand disease type 2B. *Blood*. 2005;106(9):3035-  
29 3042.
- 30 26. Groot E, de Groot PG, Fijnheer R, Lenting PJ. The presence of active von Willebrand  
31 factor under various pathological conditions. *Curr Opin Hematol*. 2007;14(3):284-289.
- 32 27. Djamiatun K, van der Ven AJ, de Groot PG, et al. Severe dengue is associated with  
33 consumption of von Willebrand factor and its cleaving enzyme ADAMTS-13. *PLoS Negl  
34 Trop Dis*. 2012;6(5):e1628.
- 35 28. Hyseni A, Kemperman H, de Lange DW, Kesecioglu J, de Groot PG, Roest M. Active  
36 von Willebrand factor predicts 28-day mortality in patients with systemic inflammatory  
37 response syndrome. *Blood*. 2014;123(14):2153-2156.

- 1 29. Chen J, Hobbs WE, Le J, Lenting PJ, de Groot PG, Lopez JA. The rate of hemolysis in  
2 sickle cell disease correlates with the quantity of active von Willebrand factor in the  
3 plasma. *Blood*. 2011;117(13):3680-3683.
- 4 30. Rutten B, Maseri A, Cianflone D, et al. Plasma levels of active Von Willebrand factor are  
5 increased in patients with first ST-segment elevation myocardial infarction: a multicenter  
6 and multiethnic study. *Eur Heart J Acute Cardiovasc Care*. 2015;4(1):64-74.
- 7 31. Chen SF, Xia ZL, Han JJ, et al. Increased active von Willebrand factor during disease  
8 development in the aging diabetic patient population. *Age (Dordr)*. 2013;35(1):171-177.
- 9 32. Zhang L, Su J, Shen F, et al. A novel monoclonal antibody against the von Willebrand  
10 Factor A2 domain reduces its cleavage by ADAMTS13. *J Hematol Oncol*.  
11 2017;10(1):42.
- 12 33. Bendetowicz AV, Wise RJ, Gilbert GE. Collagen-bound von Willebrand factor has  
13 reduced affinity for factor VIII. *J Biol Chem*. 1999;274(18):12300-12307.
- 14 34. Ulrichts H, Udvardy M, Lenting PJ, et al. Shielding of the A1 domain by the D'D3  
15 domains of von Willebrand factor modulates its interaction with platelet glycoprotein Ib-  
16 IX-V. *J Biol Chem*. 2006;281(8):4699-4707.
- 17 35. Martin C, Morales LD, Cruz MA. Purified A2 domain of von Willebrand factor binds to  
18 the active conformation of von Willebrand factor and blocks the interaction with platelet  
19 glycoprotein Ibalpha. *J Thromb Haemost*. 2007;5(7):1363-1370.
- 20 36. Van Belle E, Rauch A, Vincent F, et al. Von Willebrand Factor Multimers during  
21 Transcatheter Aortic-Valve Replacement. *N Engl J Med*. 2016;375(4):335-344.
- 22

## Legends

### Figure 1: Generation of anti-VWF nanobodies.

**A:** Flow-diagram of screening approach using recombinant VWF (rVWF) and degraded-VWF for the isolation of anti-VWF nanobodies that distinguish between intact and degraded-VWF. **B:** SDS-Agarose gel (2%) of rVWF (lane 1) and the degraded-VWF preparation (lane 2) used for screening. **C:** Coomassie-staining of an SDS-Page gel under reducing conditions containing the degraded-VWF preparation used for screening. Arrows indicate intact VWF (a) and degraded-VWF fragments (b & c), respectively. **D-F:** Dose-response of rVWF (black circles) and degraded-VWF (grey circles) to immobilized nanobody KB-VWF-D3.1 (5 µg/ml; panel D) or KB-VWF-F1.1 (5 µg/ml; panel F). Panel E compares rVWF to plasma-derived VWF (pdVWF), both added at a concentration of 5 µg/ml. Bound VWF was probed using peroxidase-labeled polyclonal anti-VWF antibodies and detected via hydrolysis of 3,3',5,5'-tetramethylbenzidine. Data represent mean±SD of 4-8 experiments.

### Figure 2: KB-VWF-D3.1 binds to the VWF A3-domain.

**A:** Binding of KB-VWF-D3.1 (1 µg/ml) to various concentrations of VWF domain-Fc fusion proteins (0-10 nM) that were captured onto anti-human Fc antibodies. Bound KB-VWF-D3.1 was probed using peroxidase-labeled polyclonal rabbit anti-cMyc antibodies and detected following hydrolysis of 3,3',5,5'-tetramethylbenzidine. A1-Fc: grey squares; A2-Fc: black triangles; A3-Fc: black circles; D4-Fc: white circles. Data represent mean±SD of 3 experiments. **B:** *In silico* simulation of KB-VWF-D3.1 (colored structures) docking on the VWF A3-domain (grey structure). Shown are the top 30-ranked structures of KB-VWF-D3.1, which all bind in a similar fashion to the A3-domain. **C:** Single structure representation of KB-VWF-D3.1 binding to the A3-domain. **D:** The VWF A3-domain, with residues in red representing amino acids predicted to be in the epitope of KB-VWF-D3.1. Residues known to affect collagen binding are indicated in yellow. **E:** Amino acid sequence of the VWF A3-domain, with the residues predicted to harbor the epitope for KB-VWF-D3.1 in red. Residues previously reported to be involved in collagen binding<sup>22</sup> are boxed. **F:** Inhibition of pd-VWF binding to collagen-type III by KB-VWF-D3.1 (closed circles), monoclonal antibody Mab505 (grey squares) and nanobody C37h (open circles). Presented is residual pd-VWF binding *versus* nanobody/antibody concentration. Data represent mean±SD of three experiments. **G:** Binding of pd-VWF (closed symbols) or degraded-VWF (open symbols) to immobilized Mab505 (5 µg/ml; circles) or C37h (5 µg/ml; squares). Bound pd-VWF was probed using peroxidase-labeled polyclonal anti-VWF antibodies and detected via hydrolysis of 3,3',5,5'-tetramethylbenzidine. Data represent mean±SD of 3 experiments.

1

2 **Figure 3: Binding of VWF with varying multimer size to KB-VWF-D3.1**

3 **A:** pd-VWF concentrates were applied to gel-filtration chromatography using Bio-Gel-A-15m.  
4 Fractions enriched in high molecular weight-multimers (HMW-VWF) and medium molecular  
5 weight-multimers (MMW-VWF) were analyzed for their multimeric pattern using SDS-  
6 agarose (2%) electrophoresis. **B:** Binding of HMW-VWF (closed circles) and MMW-VWF  
7 (open circles) to immobilized KB-VWF-D3.1 (5 µg/ml). **C.** Binding of multimeric rVWF (closed  
8 circles) and the dimeric VWF/delta-pro variant (grey squares) to immobilized KB-VWF-D3.1  
9 (5 µg/ml). In both panels, bound VWF was probed using peroxidase-labeled polyclonal anti-  
10 VWF antibodies and detected via hydrolysis of 3,3',5,5'-tetramethylbenzidine. Data represent  
11 mean±SD of 3-4 independent measurements.

12

13 **Figure 4: ADAMTS13-mediated proteolysis modulates binding of VWF to KB-VWF-**  
14 **D3.1 and KB-VWF-F1.1.**

15 **A:** Purified pd-VWF was incubated with recombinant ADAMTS13 and exposed to vortex-  
16 induced shear. Samples taken at indicated time-points (0-3h) were analyzed via SDS-  
17 agarose electrophoresis. As a control, pd-VWF was exposed to ADAMTS13 and shear for 3  
18 h in the presence of EDTA, a chelating agent that blocks ADAMTS13 activity. **B:** Samples  
19 were analyzed for total VWF-antigen using polyclonal antibodies, for the presence of intact-  
20 VWF using KB-VWF-D3.1 and for the presence of degraded-VWF using KB-VWF-F1.1.  
21 Presented is the ratio intact-VWF/total VWF-antigen (closed circles; left Y-axis) and the ratio  
22 degraded-VWF/total VWF-antigen (grey squares; right Y-axis) versus exposure time to  
23 ADAMTS13. Normal pooled plasma was used as calibrator for KB-VWF-D3.1, whereas a  
24 degraded-VWF preparation was used as calibrator for KB-VWF-F1.1. Data represent  
25 mean±SD of 3 independent experiments.

26

27 **Figure 5: Detection of intact VWF in congenital VWD**

28 **A:** VWF-deficient plasma was spiked with different amounts of purified rVWF and degraded-  
29 VWF, and incubated in microtiter plates coated with KB-VWF-D3.1. Bound VWF was probed  
30 using peroxidase-labeled polyclonal anti-VWF antibodies and detected via hydrolysis of  
31 3,3',5,5'-tetramethylbenzidine. Data represent mean±SD of 3-4 independent measurements.  
32 The solid line illustrates the best linear fit, with 95% confidence interval indicated with the  
33 dotted lines. The vertical line indicates 90% intact rVWF supplemented with 10% degraded-  
34 VWF **B-C:** Patient plasma samples were analyzed for total antigen using polyclonal  
35 antibodies and for intact-VWF using KB-VWF-D3.1. Normal pooled plasma was used as  
36 calibrator. Presented is the ratio intact-VWF/total VWF-antigen. Each individual sample is



1 represented by a closed symbol. Statistical analysis was performed via a one-way Anova  
2 with Dunnett's correction for multiple comparisons (*panel B*) or Mann-Whitney (*panel C*). **D:**  
3 Multimers were analyzed via SDS-agarose electrophoresis. The relative amount of  
4 multimers exceeding 10 bands was determined via comparison to normal pooled plasma  
5 (NPP). **E:** Plotted is the ratio intact-VWF/total VWF-antigen *versus* the relative amount of  
6 large multimers. Correlation was determined in using Graphpad Prism Software.

7

#### 8 **Figure 6: Detection of intact VWF in AVWS**

9 **A:** Multimers were analyzed via SDS-agarose electrophoresis. The relative amount of  
10 multimers exceeding 10 bands was determined via comparison to normal pooled plasma  
11 (NPP). **B:** Patient plasma samples were analyzed for total antigen using polyclonal  
12 antibodies and for intact-VWF using KB-VWF-D3.1. Normal pooled plasma was used as  
13 calibrator. Presented is the ratio intact-VWF/total VWF-antigen. Each individual sample is  
14 represented by a closed symbol. Statistical analysis was performed via a one-way Anova  
15 with Dunnett's correction for multiple comparisons. Control samples were identical to those  
16 presented in Figure 5. **C-D:** Plotted is the ratio intact-VWF/total VWF-antigen *versus* the  
17 relative amount of large multimers for samples from patients with severe aortic stenosis (AS;  
18 *panel C*) and from ECMO patients (*panel D*).

19

20

# Figure 1

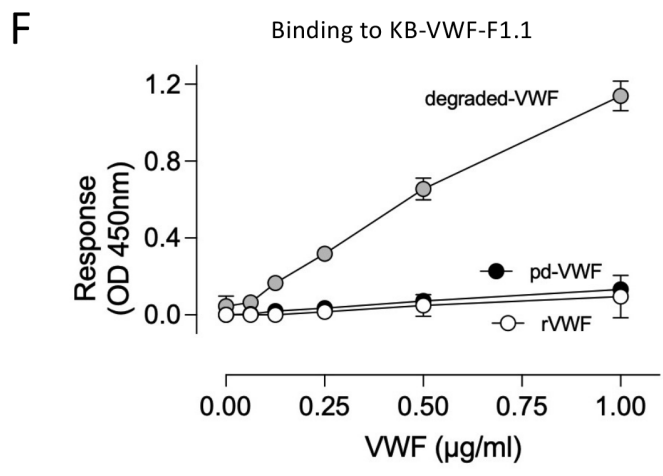
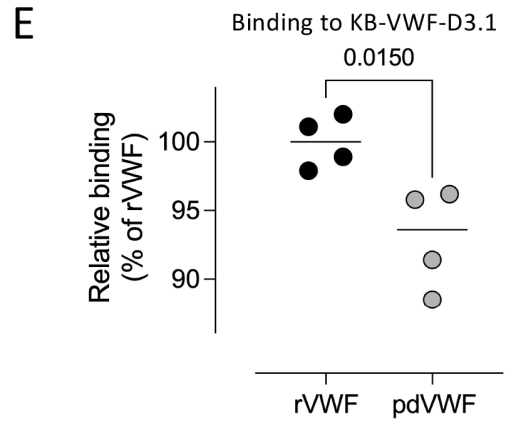
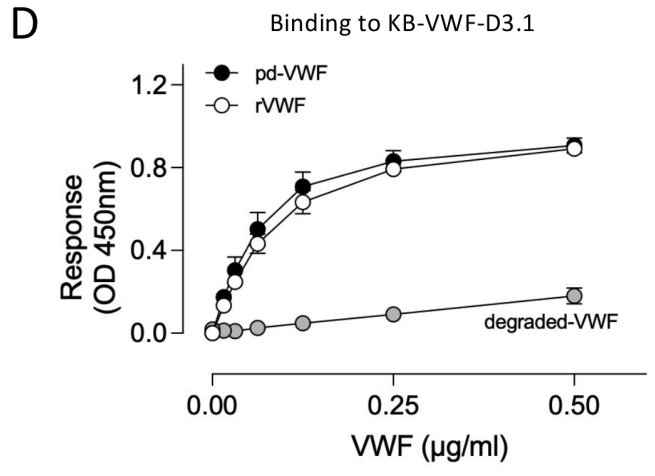
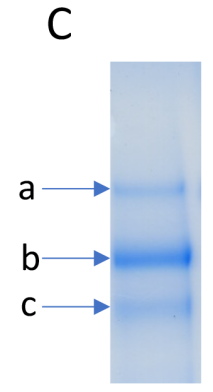
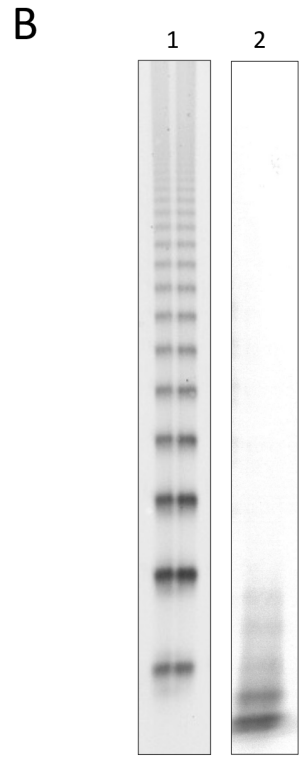
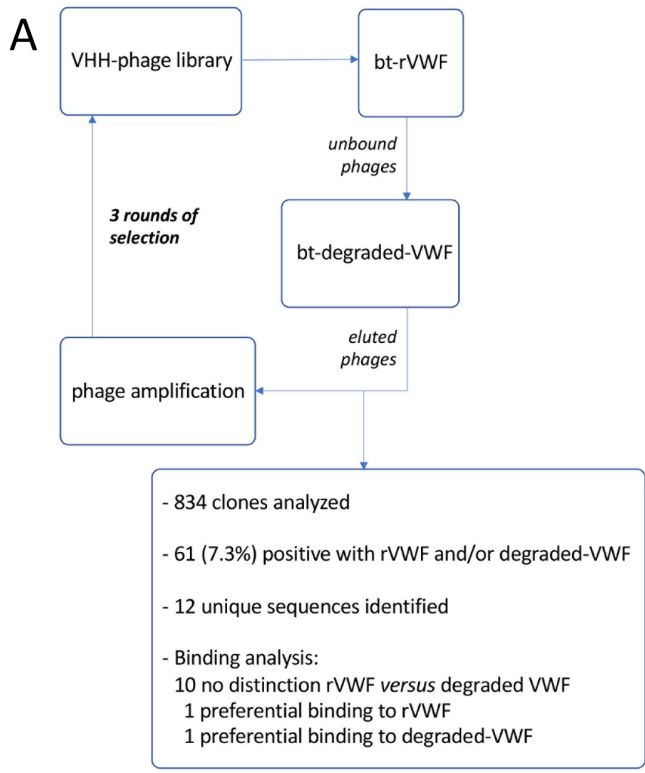


Figure 2

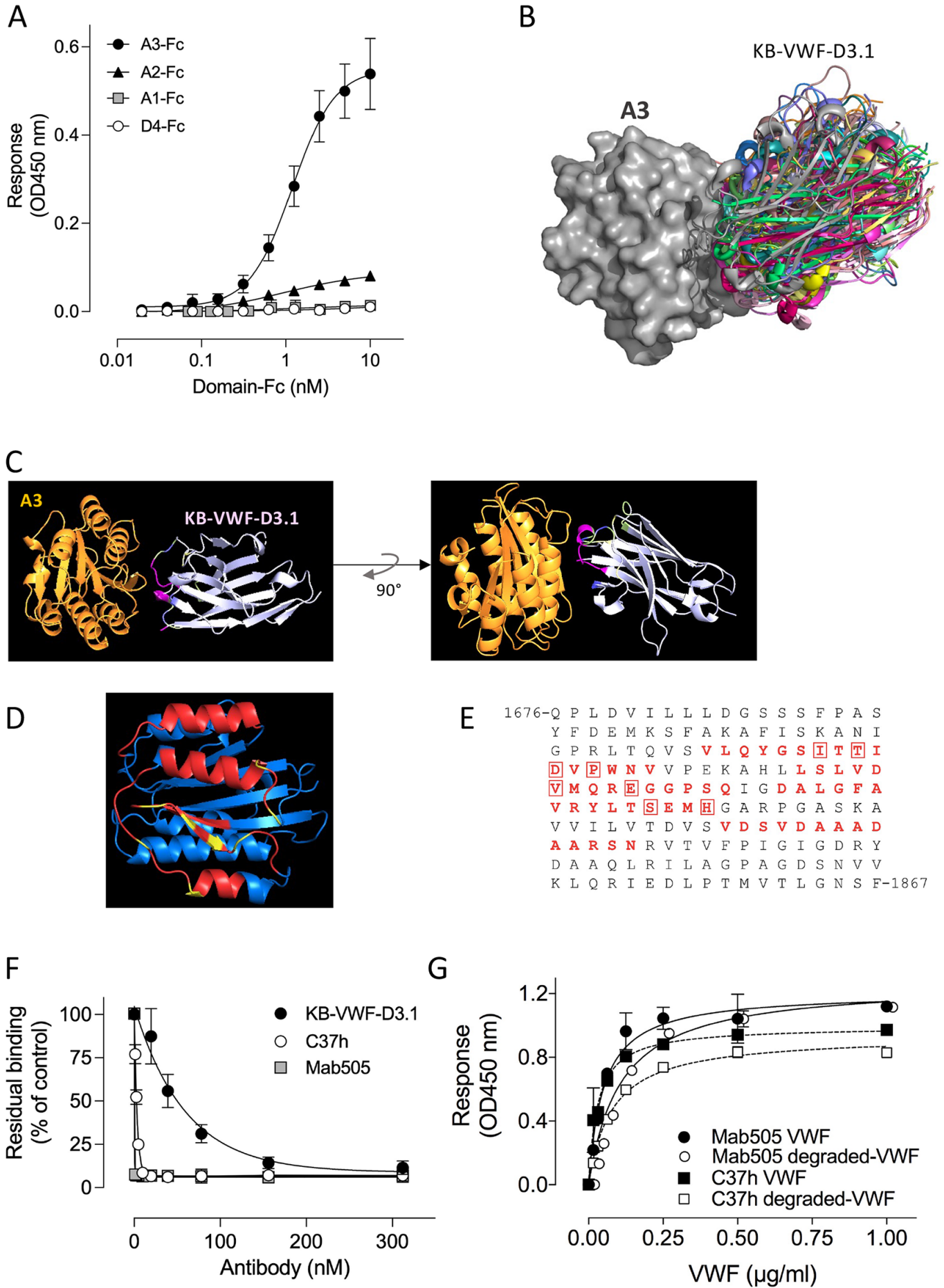


Figure 3

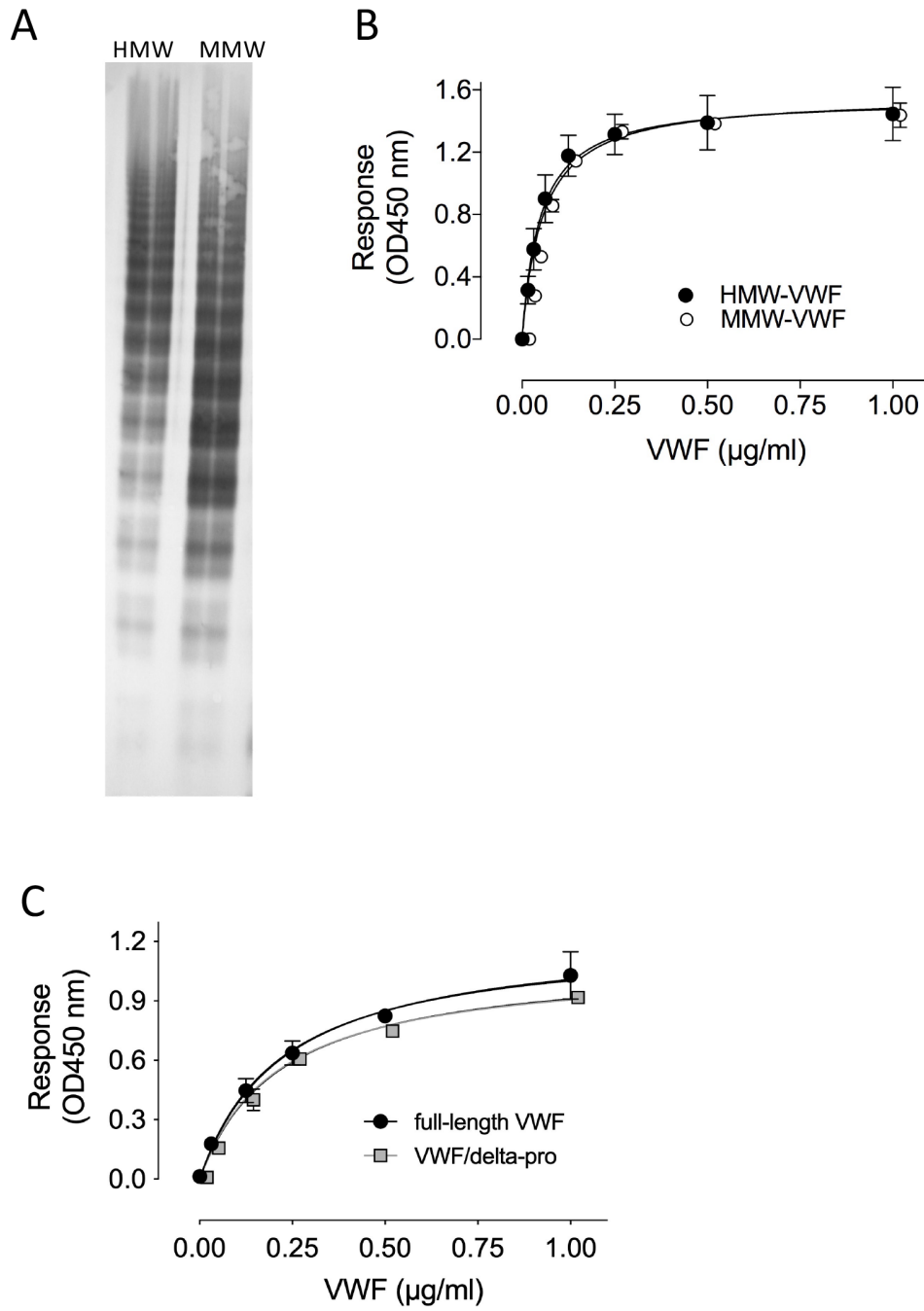
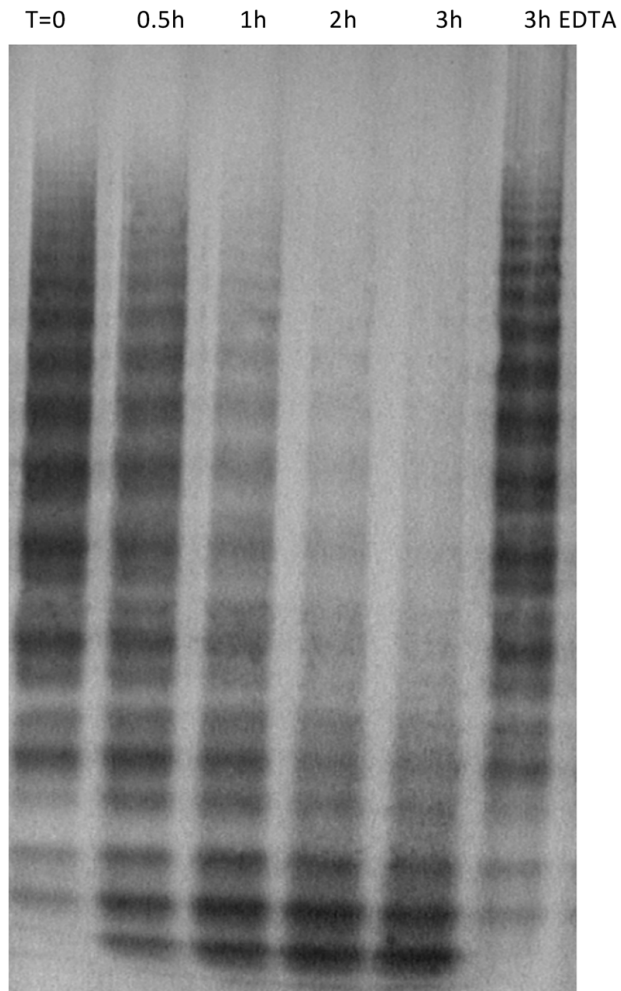


Figure 4

A



B

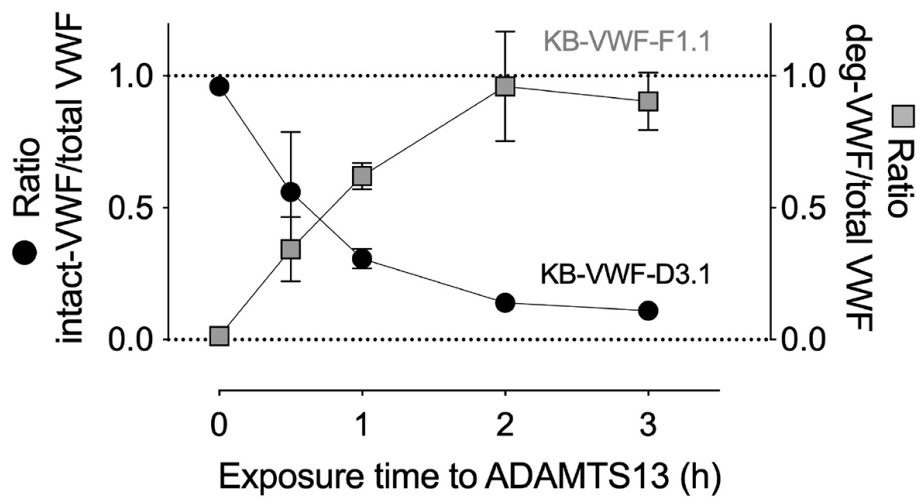


Figure 5

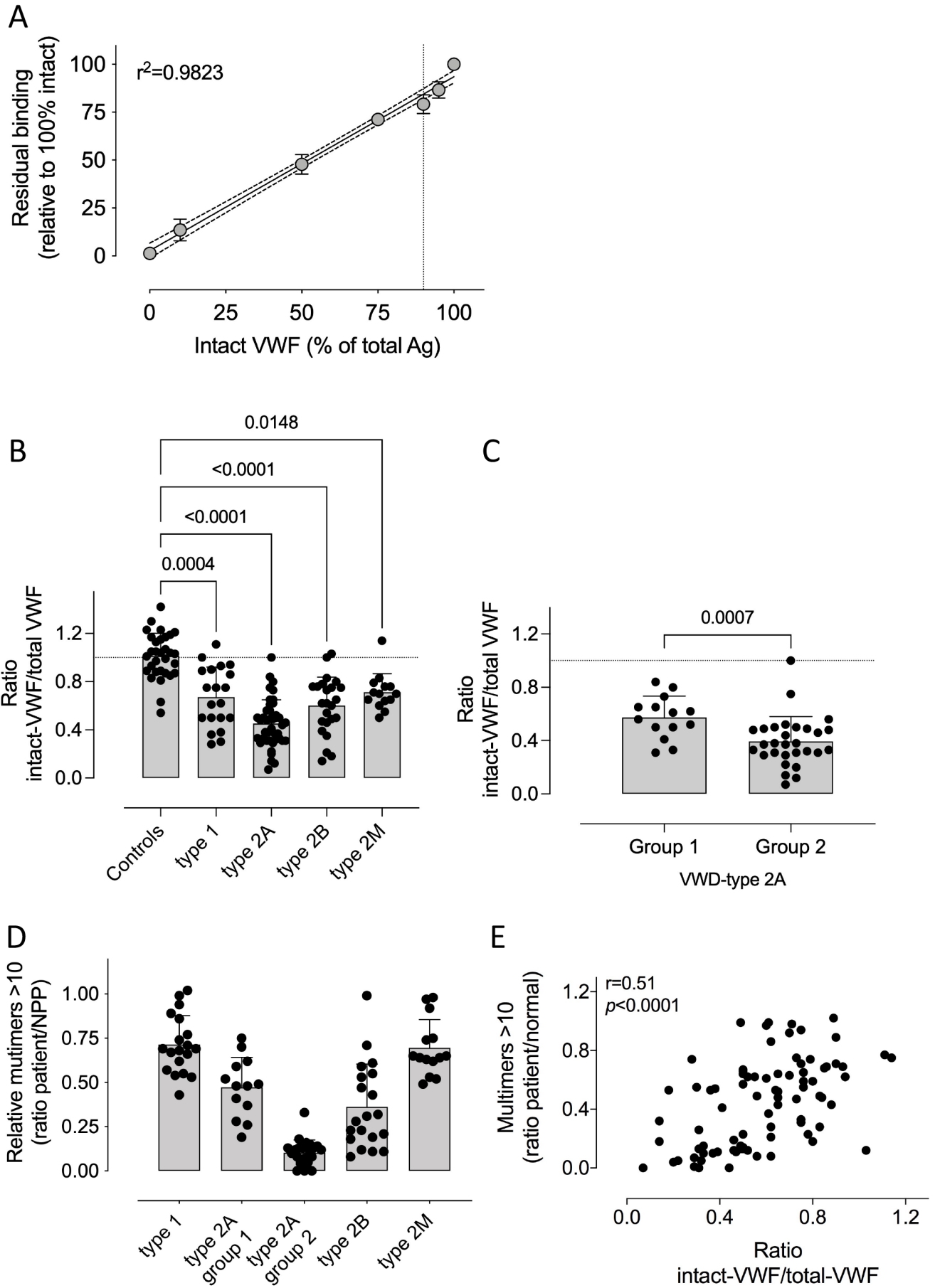


Figure 6

